2016 International Conference on Indoor Positioning and Indoor Navigation (IPIN), 4-7 October 2016, Alcalá de Henares, Spain

Work in Progress: Combining Indoor Positioning and 3D Point Clouds from Multispectral Lidar

Sanna Kaasalainen, Simo Gröhn, and Laura Ruotsalainen
Finnish Geospatial Research Institute – FGI
Department of Navigation and Positioning
Masala, Finland
firstname.lastname@nls.fi

Olli Nevalainen, Teemu Hakala
Finnish Geospatial Research Institute – FGI
Department of Remote Sensing and Photogrammetry
Masala, Finland
firstname.lastname@nls.fi

***Abstract*— We have studied the potential of combining multispectral Light Detection And Ranging (lidar) with positioning sensors to produce spatially resolved target identification in indoor environment. There is a growing need for automatic and mobile mapping and surveillance in buildings and locations where satellite positioning is not available. Lidar has proven a useful tool in distance measurements and is being used in Simultaneous Localization and Mapping (SLAM) as a range sensor. The recent advances in multispectral lidar technology will improve the laser-based object recognition and enable a new level of autonomous surveillance in the near future.**

Keywords*— *Hyperspectral Sensors, Lidar, Navigation, Remote Sensing

I. INTRODUCTION

Light detection and ranging (lidar) is increasingly being used in simultaneous location and mapping (SLAM) applications. SLAM applications typically combine lidar with odometry sensors, Inertial Measurement Units (IMU), and Global Navigation Satellite System (GNSS) [1].

Thus far the majority of mobile laser scanning systems have been based on GNSS [2], but the increasing need for indoor applications will emphasize the role of multi-sensor indoor positioning [3,4].

Simultaneous Localization and Mapping (SLAM) provides infrastructure-free accurate and reliable localization and information on the environment by means of adaptive integration of data from multiple sensors (e.g., [4,5,6]).

The common estimation frameworks to produce a SLAM solution are based on Kalman filter (KF) and particle filter (PF) [4]. PF was implemented in [7] to integrate motion measurements from a monocular camera, foot-mounted Inertial Measurement Unit (IMU), Sound Navigation And Ranging (sonar), and barometer to produce an accurate and reliable localization solution for use in SLAM. They obtained horizontal accuracy of 3.14 m with standard deviation of 2.82 m for the localization solution and called for more accurate error modeling and additional sensors, such as multiple IMU's, to improve the results.

Trade-off between accuracy and time cost (related to computing efficiency and, e.g., image processing and feature extraction) is characteristic to indoor SLAM solutions [5]. Centimeter-level accuracy has been achieved with methods based on post processing, while a real-time application could be improved to decimeter level at least for feature-rich environments [8]. This emphasizes the need for new sensors to improve the efficiency of real-time SLAM.

In the past few years, laser scanning (scanning lidar) applications have reached a new level as multi-wavelength lidar applications have emerged [9,10,11]. These new developments have significantly increased the information content in lidar point clouds and enabled a new level of detail in, e.g., vegetation studies, where hyperspectral sensing is a well-established method for identification and classification of targets [12,13,14]. Active hyperspectral sensing based on supercontinuum lasers has also been applied indoors for distinguishing different targets, both inorganic and vegetation [15,16].

The aim of the research presented in this paper is to enhance the lidar-based indoor mapping with a multispectral target identification aspect. Our aim is to combine multispectral 3D point clouds and point-wise target identification from lidar with indoor positioning sensors, such as sonar and IMU, to produce an indoor mapping method for localizing different phenomena, such as humidity or mold in building structures. This would enable the use of indoor SLAM not only for navigation of an autonomous vehicle but also for autonomous surveillance in, e.g., security applications.

This work in progress paper is organized as follows: the multispectral lidar approach and the experiments are described in Sect. II. The preliminary experimental results are presented in Sect. III, and the conclusions and forthcoming work are summarized in Sect. IV.

II. II. MULTISPECTRAL LIDAR MEASUREMENT

The FGI hyperspectral lidar (HSL) was used in the experiment. The first prototype of the lidar was built in 2012 [9] and later modified for improved field operation and sensors. The operating principle is similar to a conventional pulse-based terrestrial laser scanner, except that supercontinuum laser

source [16] (41 mW average optical power, 5 kHz pulse rate) was used instead of a monochromatic laser. An off-axis parabolic mirror was used as a primary optic to gather the return pulses. A spectrograph (Specim ImSpector V10) was placed in front of the detector (avalanche photodiode, APD) to obtain a spectrum for the returning laser pulse. The APD array comprises 16 channels, but as an 8-channel digitizer (1 GHz) was used, the return intensity could only be recorded in 8 wavelengths. Thus, in spite of the hyperspectral light source, the detector system is multispectral, but the wavelength channels can be selected by adjusting the spectrograph position. A monochromator (Oriel, Cornerstone 74125) was used to calibrate the spectral responses of the APD elements. A 2D scanner was used to scan over the target and to produce a point cloud. See Fig. 1 and [9] for more details on the instrument and data processing.

Fig. 2 shows an example of target identification with the HSL using spectral libraries. Spectral libraries also enable the classification of each point using the spectral features, which will enable faster (real-time) detection than that based on 3D features derived from the point cloud (e.g., during post-processing).

The targets were placed hanging on a wire in the middle of the area to be scanned. Three different targets were investigated: two cardboard samples (one wet and one dry) and a wooden panel with some moist on it (see Fig. 3).

The wavelength channels in this study were 536, 589, 634, 688, 741, 793, 848, and 951 nm. We scanned the entire corner of the laboratory to produce a point cloud larger than the samples to demonstrate how the point cloud can be applied for the location of the samples in the room. The HSL point clouds where processed with MATLAB 2013a software (The MathWorks®, Inc). The cardboard and wood samples were manually cropped from the point cloud to obtain the mean backscattered reflectance of all the echoes from each target.

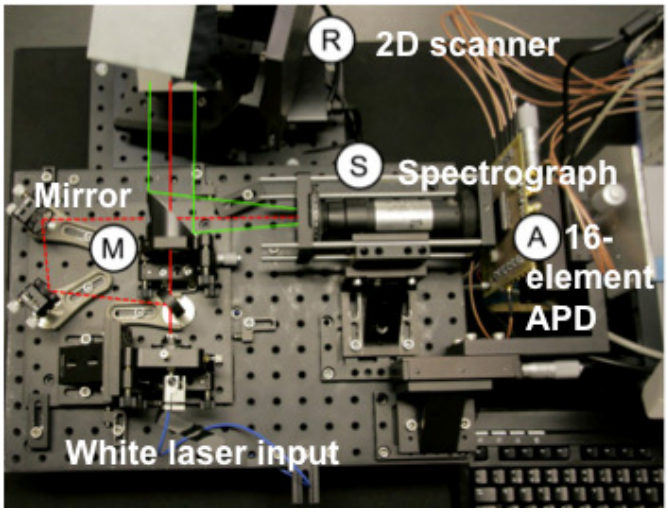

Fig. 1. The FGI hyperspectral lidar (HSL) optical setup: Red beam: White laser input. R: 2D scanner. M: Off-axis parabolic mirror. S: Spectrograph. A: 16 element avalanche photo diode array.

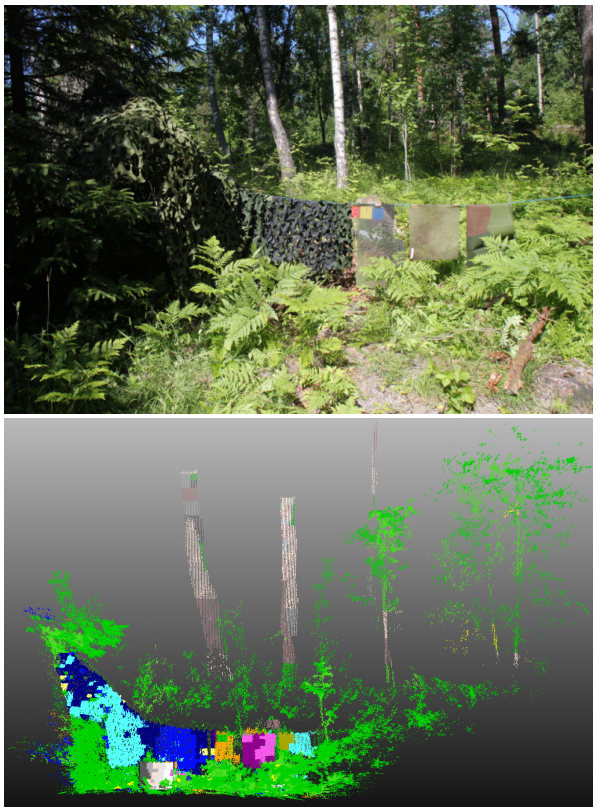

Fig. 2. Target identification with the FGI hyperspectral lidar (HSL), showing the capability of the instrument of detecting targets in the scanned area using spectral libraries.

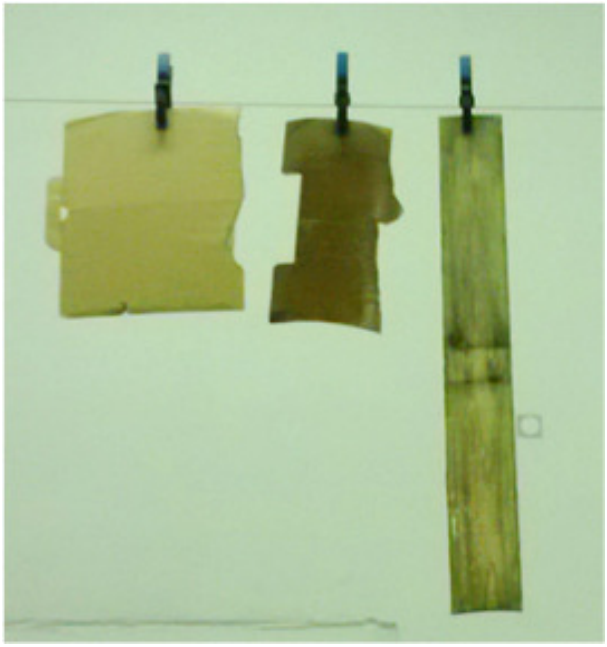

Fig. 3. The targets hanged on a wire in the scanned area. The wet and dry cardboard samples are in the left and middle, respectively.

III. Experimental Results

These results are preliminary, but they enable us to explore qualitatively the ability of our instrument to distinguish between wet and dry inorganic targets.

A. *Point Clouds*

The point cloud of the scanned laboratory corner and the targets is shown in Fig. 4. Fig. 5 shows a close-up of the targets and their intensity in 848 nm. The difference in the intensity between different targets is visible at all wavelengths.

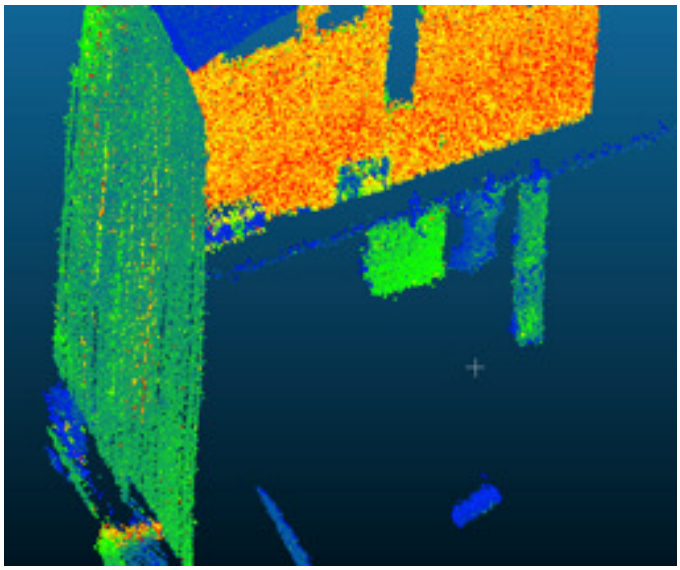

Fig. 4. The HLS point cloud (plotted with CloudCompare Version: 2.6.1) of the laboratory corner with the targets visible in the middle of the image. The point cloud is shown with intensity in one of the Near-Infrared channels.

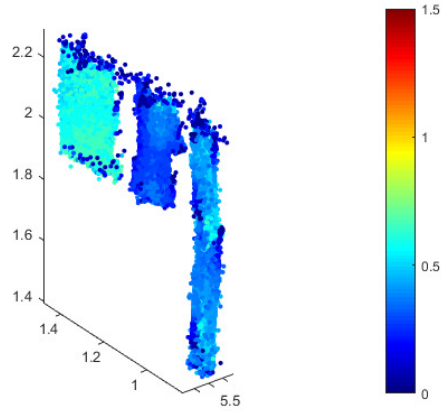

Fig. 5. The targets cropped from the original point cloud. The intensity for each point is plotted in HSL channel 7: 848 nm. The wet and dry cardboard samples are in the left and middle, respectively (cf. Fig. 3).

B. *Spectra*

The spectra of the wet and dry cardboard panel are plotted in Fig. 6. There is a clear difference in the intensity in all channels. This difference is more pronounced at NIR wavelengths greater than 1000 nm because of the strong water absorption lines at 1400 nm and 1900 nm, which could be used for water detection [e.g., 15].

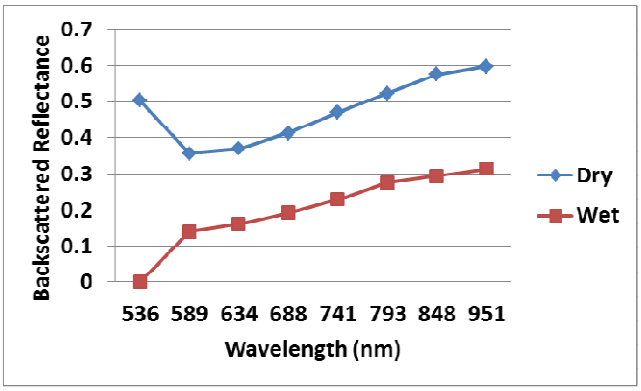

Fig. 6. The 8-channel spectra of the wet and dry cardboard targets.

To demonstrate the potential for mapping the spectral indices, we have also plotted a point cloud showing the water concentration index [17], which is based on a water absorption band at 970 nm and a reference wavelength (900 nm) in Fig. 7. The water index used in this study is defined as:

$$WI = \frac{R_{900}}{R_{970}} \quad (1)$$

As 900nm and 970 nm were not available in this measurement, we used 848 nm and 951 nm instead (cf. [9]). Even though the water absorption is stronger at wavelengths further in the near-infrared, the difference between the wet and dry cardboard samples is already visible in the point cloud.

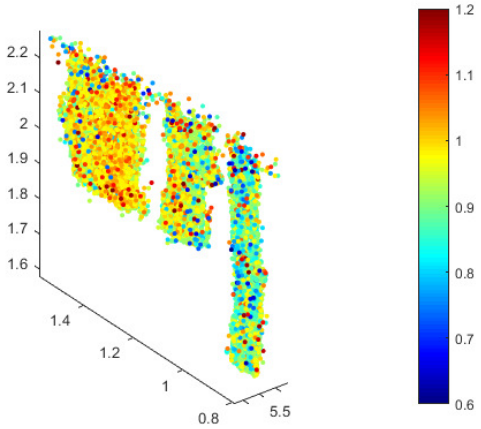

Fig. 7. The targets cropped from the original point cloud showing the water index R848/R951 (cf. Eq. 1) for each point.

IV. IV. CONCLUSION AND FUTURE WORK

In our earlier studies we have shown that the HSL is capable of detecting leaf-level moisture in vegetation and its distribution over a large target [9]. We have also shown the feasibility of the HSL in classifying targets with both spectral and spatial features (Fig. 2). By carrying out a similar experiment for industrial cardboard and wood samples, we aimed at demonstrating the prospects of extending this methodology to built environment. Combining the

hyperspectral lidar detection with positioning sensors would enable both real-time SLAM with improved optical sensing (e.g., point wise target identification using spectral libraries) and autonomous indoor mapping (with, e.g., unoccupied ground vehicles or other robotic platforms) and using the post-processed 3D point cloud data in surveillance and other monitoring applications to identify targets of interest and producing indoor maps.

Knowing from other studies (e.g., [15]) and preliminary experiments that water absorption in the NIR has a stronger effect on reflection than in our measurements, one of the aims of our future study is to extend the wavelength range of our instrument to cover the optical infrared bands for improved water and moisture detection.

ACKNOWLEDGMENT

This study was financially supported by the following projects: INTACT (INfrastructure-free TACTical situational awareness), funded by the Scientific Advisory Board for Defence of the Finnish Ministry of Defence and the Finnish Geospatial Research Institute (FGI), Finland, and TEKES (the Technology Development Center of Finland) project 1515/31/2016: 'Efficient and safe identification of minerals: smart real-time methods'.

REFERENCES

[1] F. Mutz, L. P. Veronese, T. Oliveira-Santos, E. de Aguiar, F. A. Auat Cheein, and A. Ferreira De Souza, "Large-scale mapping in complex field scenarios using an autonomous car," *Expert Systems with Applications*, vol. 46, pp. 439–462, Mar. 2016.

[2] D. Barber, J. Mills, and S. Smith-Voysey, "Geometric validation of a ground-based mobile laser scanning system," *ISPRS Journal of Photogrammetry and Remote Sensing*, vol. 63, no. 1, pp. 128–141, Jan. 2008.

[3] N. Haala, D. Fritsch, M. Peter, and A. M. Khosravani, "Pedestrian Mobile Mapping System For Indoor Environments Based On MEMS IMU And Range Camera," Archives of Photogrammetry, Cartography and Remote Sensing, vol. 22, pp. 159-172, Dec. 2011.

[4] Z. Riaz, A. Pervez, M. Ahmer, and J. Iqbal, "A fully autonomous indoor mobile robot using SLAM,", in *International Conference on Information and Emerging Technologies (ICIET)*, Karachi, 2010, pp. 1–6.

[5] Z. Chen, J. Samarabandu, and R. Rodrigo, "Recent advances in simultaneous localization and map-building using computer vision, " *Advanced Robotics,* vol. 21, no. 3-4, pp. 233-265, 2007.

[6] H. Durrant-Whyte and T. Bailey, "Simultaneous Localisation and Mapping (SLAM): Part I The Essential Algorithms," *Robotics & Automation Magazine*, vol. 13, no. 2, pp. 99-110, 2006.

[7] L. Ruotsalainen, S. Grohn, M. Kirkko-Jaakkola, L. Chen, R. Guinness, and H. Kuusniemi, "Monocular visual SLAM for tactical situational awareness," *Indoor Positioning and Indoor Navigation (IPIN), 2015 International Conference on*, Banff, AB, 2015, pp. 1-9.

[8] J. Tang, Y. Chen, A. Jaakkola, J. Liu, J. Hyyppä, and H. Hyyppä, "NAVIS-An UGV Indoor Positioning System Using Laser Scan Matching for Large-Area Real-Time Applications," *Sensors*, vol. 14, no. 7, pp. 11805–11824, Jul. 2014.

[9] T. Hakala, J. Suomalainen, S. Kaasalainen, and Y. Chen, "Full waveform hyperspectral LiDAR for terrestrial laser scanning," *Optics Express*, vol. 20, no. 7, p. 7119, Mar. 2012.

[10] E. S. Douglas, J. Martel, Zhan Li, G. Howe, K. Hewawasam, R. A. Marshall, C. L. Schaaf, T. A. Cook, G. J. Newnham, A. Strahler, and S. Chakrabarti, "Finding Leaves in the Forest: The Dual-Wavelength Echidna Lidar," *IEEE Geoscience and Remote Sensing Letters*, vol. 12, no. 4, pp. 776–780, Apr. 2015.

[11] L. A. Schofield, F. M. Danson, N. S. Entwistle, R. Gaulton, and S. Hancock, "Radiometric calibration of a dual-wavelength terrestrial laser scanner using neural networks," *Remote Sensing Letters*, vol. 7, no. 4, pp. 299–308, Apr. 2016.

[12] R. Gaulton, F. M. Danson, F. A. Ramirez, and O. Gunawan, "The potential of dual-wavelength laser scanning for estimating vegetation moisture content," *Remote Sensing of Environment*, vol. 132, pp. 32–39, May 2013.

[13] W. Li, G. Sun, Z. Niu, S. Gao, and H. Qiao, "Estimation of leaf biochemical content using a novel hyperspectral full-waveform LiDAR system," *Remote Sensing Letters*, vol. 5, no. 8, pp. 693–702, Aug. 2014.

[14] O. Nevalainen, T. Hakala, J. Suomalainen, R. Mäkipää, M. Peltoniemi, A. Krooks, and S. Kaasalainen, "Fast and nondestructive method for leaf level chlorophyll estimation using hyperspectral LiDAR," *Agricultural and Forest Meteorology*, vol. 198–199, pp. 250–258, Nov. 2014.

[15] A. Manninen, T. Kääriäinen, T. Parviainen, S. Buchter, M. Heiliö, and T. Laurila, "Long distance active hyperspectral sensing using high-power near-infrared supercontinuum light source," *Optics Express*, vol. 22, no. 6, p. 7172, Mar. 2014.

[16] D. A. Orchard, A. J. Turner, L. Michaille, and K. R. Ridley, "White light lasers for remote sensing," 2008, p. 711506.

[17] J. PeñUelas, I. Filella, C. Biel, L. Serrano, and R. Savé, "The reflectance at the 950–970 nm region as an indicator of plant water status," *International Journal of Remote Sensing*, vol. 14, no. 10, pp. 1887–1905, Jul. 1993.